Effects of irregular sampling on 3-D prestack migration

Gerald H.F. Gardner* and Anat *Canning, Houston Advanced Research Center*

Summary

In a direct application of Kirchhoff migration each trace is added to the migrated volume by spreading the data along impulse response curves with suitable change in the amplitude and shape of the wavelets. Overlapping impulse responses form the correct answer where they form an envelope and are supposed to cancel elsewhere. For uniform data (constant offset, constant azimuth, constant midpoint spacing and constant velocity) the cancellation is excellent and the reflectors have the correct amplitude. This paper shows how failure to meet any of these constancy criteria results in noise. Modified summation procedures can reduce the noise at the expense of a loss of resolution.

Introduction

Multi-fold 3-D surveys are often designed to facilitate stacking by arranging that many traces have midpoints close to a regular grid. The grid spacing is made as large as is reasonable to obtain a high fold. It is somewhat disconcerting to find that prestack Kirchhoff migration of such data may produce a noisier result than DMO, stack and migration. We illustrate this possibility using the coordinates from a land survey and synthetic data.

The noise created by Kirchhoff summation can be coherent and have the appearance of reflections, or it may just obscure the correct images. One cause of the noise is too large a trace spacing, which leads to operator aliasing. Lumley et al. (1994) have shown that for regular trace spacing it is possible to design an operator filter that effectively reduces the noise, but their analysis does not apply to irregular trace spacing. We show in this paper that noise is also created by variations in offset or azimuth from one trace to the next, even when the midpoint spacing is regular and small. Because 3-D surveys contain irregular variations in midpoint, offset and azimuth we propose that the degree of filtering required can be determined empirically by applying a modified Kirchhoff surnmation using the actual coordinates of the survey and suitable synthetic data.

The survey layout

All the basic distances in the layout are multiples of 100 A. There are 16 N-S receiver lines with a separation of 1320 ft and 8 E-W shot lines with a separation of 2640 A. Along the receiver lines the geophone station interval is 220 ft, and along the shot lines the vibrator station interval is 440 ft. There are three shots symmetrically placed between adjacent receiver lines. All receivers within 5280 ft of a shot in the E-W direction, and within 9240 ft of a shot in the N-S direction, are active for each shot. Thus, at most 8 N-S lines are active at any one time, with 84 receivers on each line. Because the distances are multiples of 110, all the midpoints lie on a grid 110 ft in the N-S direction, by 220 ft in the E-W direction. The fold varies from one at the edge to about 25 at the center.

In the actual field implementation of this design, many vibrator points were displaced from the planned positions because of obstacles. The total number of traces was 250,000 in an area 19800 ft by 19800 ft (14 square miles). Figure 1 shows a plot of the actual VP stations and the actual receiver stations. As a result of this design, offset and azimuth vary from one midpoint to the next. The departures from the plan add more irregularities to the trace distribution.

Comparison of post-stack and prestack migration

To test the adequacy of the layout design, synthetic data were generated with this layout and processed in two ways. First, 3-D DMO was applied, followed by stack and migration; second, 3-D prestack Kirchhoff migration was applied. The synthetic data corresponded to a model with three horizontal interfaces at depths of 2000, 4000 and 6000 A, with equal reflection coefficients independent of the angle of incidence. The wavelet was one complete cycle defined by $\sin(2\pi ft) - 0.5 \sin(4\pi ft)$, where $f = 15$ Hz and the beginning of the wavelet marks the reflection. The maximum frequency was about 40 Hz. The velocity was constant and equal to 11000 ft/sec. For this velocity and maximum frequency the sampling interval for migration $v/4 f_{max}$, is about 66 ft.

Theoretically, because the velocity is constant, post-stack and prestack migration should yield identical results, whatever the data. However, the 3-D DMO applied in these tests has midpoint and offset filters embedded in the procedure, whereas the 3-D Kirchhoff migration does not.

The input data were not muted, nor were any weighting factors applied to correct for irregularities in the spacing. Thus there is considerable stretching of the wavelet for the large offsets (~11,000 ft) and shallowest interface (2,000 A). Nevertheless, the post-stack and prestack migrations should be identical.

Figures 2 and 3 show the results of post-stack and prestack migration for a N-S line as indicated in Figure 1. It is evident that the prestack migration is noisier. The post-stack migration is quite free of background noise, the wavelet is well-preserved, and the amplitude variation is smooth, increasing toward the center of the survey as the fold increases. In contrast, the prestack data show migration smiles, the wavelet is distorted and the amplitude is erratic.

3-D DMO

The result of the 3-D DMO followed by stack is shown in Figure **4.** This shows that the smoothing of the data occurs at this step. The velocity-independent DMO was done by applying a log-stretch to the input traces, taking an FFT of each input trace, multiplying each frequency component by a filter factor for each replacement point between the shot and receiver, adding into the four grid points nearest to the midpoint and into the two offsets nearest to the new offset. Since no NMO was applied, the filtering effect of this summation procedure increases as offset increases. An inverse FFT and log-stretch restores the data to the time domain.

3-D Kirchhoff Migration

In the Kirchhoff migration each trace was added to the answer using an obliquity factor based on the offset of the trace, i.e., as if the trace were part of a constant-offset, constant azimuth, survey. The formula for the summation is

$$A(Q,t) = \left(\frac{1}{\pi}\right)\left(\frac{2}{v}\right)dxdy \sum_{all\ traces}\left(\frac{t}{T}\right)\left(\frac{1+\sigma^2}{\left(1-\sigma^2\right)^2}\left|\frac{d}{dt}(data)\right|_{@T}\right)$$

where

t = output time at output depth point Q ,

σ = $(t_r - t_s)/(t_r + t_s)$,

t_r = travel time from receiver to Q ,

t_s = travel time from shot to Q ,

T = $t_r + t_s$.

Velocity Analysis and AVO Analysis

Another comparison of Kirchhoff summation and DMO-PSI can be made by looking at CMP gathers after imaging but before stack. Figure 5a shows a gather using Kirchhoff summation to accumulate migrated traces by the offset of the original trace (common image gather); Figure 5b shows the gather after DMO + PSI + NMO; and Figure 5c shows an ideal result using constant-offset, constant azimuth traces with midpoints on a regular grid. It is clear that the irregularity of the coordinates makes Kirchhoff summation much noisier than the DMO-PSI process. This example shows that the effect of irregularities is more severe in the prestack domain and may cause problems with velocity analysis and with AVO analysis.

Examples of operator aliasing

Figures 6a - 6d illustrate some operator aliasing problems. First, for a single-fold, constant offset (2,000 R), constant azimuth, small regular spacing (55 R), Kirchhoff migration gives an almost noise-free result as shown in Figure 6a. The wavelet and model are the same as for the previous examples; the output trace spacing is 55 ft in all the examples.

Aliasing is introduced if the offset is changed from trace to trace. In this case, the coverage was obtained by having 16 receivers in a square array with spacing 110 ft record a shot at a distance from the array of 2000 ft. This template was moved over shot positions on a square grid with spacing 220 ft (Figure 7). The result is single-fold with midpoints at 55 ft and offsets between 2000 ft and 2400 ft from one midpoint to the other (Figure 6b). Even this small a variation in offset produces a visible background noise.

As another example, the same template was used, but with a receiver spacing of 990 ft and a shot offset of 1000 ft. Again, the midpoint spacing is 55 ft but the jumps in offset are large. The noise level is increased by the increase in offset variability, as show in Figure 6c. A fine midpoint spacing by itself does not guarantee a noise-free image.

On the other hand, the noise resulting from a coarse grid spacing (Figure 6e) is diminished by a high fold. If the receiver grid spacing is changed to 880 ft the midpoint spacing becomes 220 ft and there are 16 traces at each midpoint. Figure 6d shows the result: the noise level is about the same as in Figure 6c.

Finally, Figure 6e shows one-fold data on a 220 x 220 ft grid with a constant offset of 1000 ft. Here offset does not vary, but midpoint spacing is much too large and therefore aliasing noise is large. It creates events that could be mistaken for horizontal reflectors.

Conclusions

Examples of Kirchhoff prestack migration show that operator aliasing creates noise whenever the spacing is too large. When the offset is not constant, or the azimuth varies (for dipping reflectors) aliasing noise increases. The design of an operator filter to attenuate these effects will be discussed in the oral presentation.

References

Lumley, D. E., Claerbout, J. F. and Beve, D., 1994, *Anti-aliased Kirchhoff 3-D migration,* 64th Ann. Intemat. Mtg., Soc. Expl. Geophys., Los-Angeles.
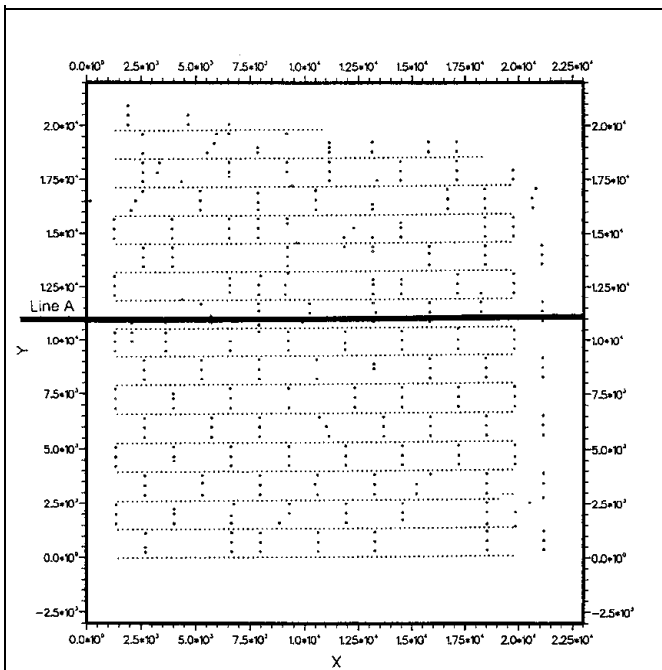
Acknowledgment

Fig. 1. Layout of the 3-D survey. Shot locations are marked with "₀" ; receiver locations are marked with "•"; line A mark the position of the section that is presented in the following Figures.
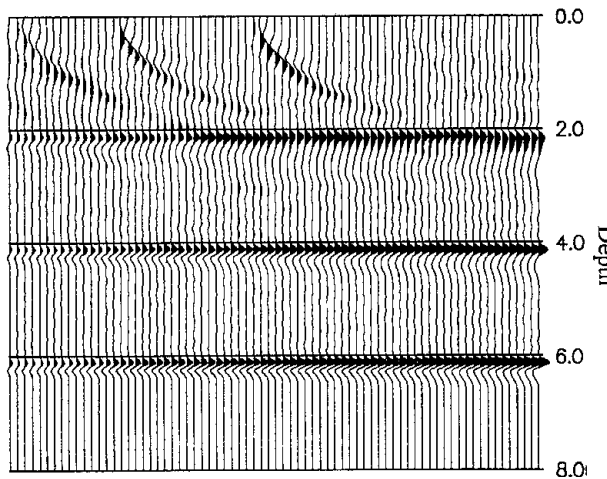

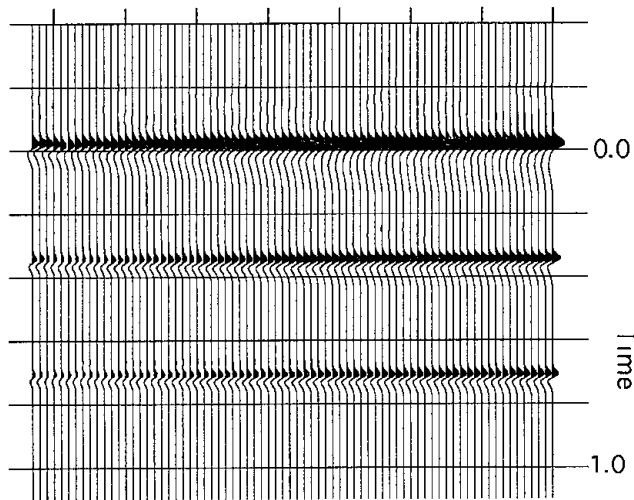Fig. 3. Result of 3-D DMO and migration using the coordinates of the real 3-D survey (@ line A).

Fig. 2. Result of 3-D prestack migration using the coordinates of the real 3-D survey (@ line A).
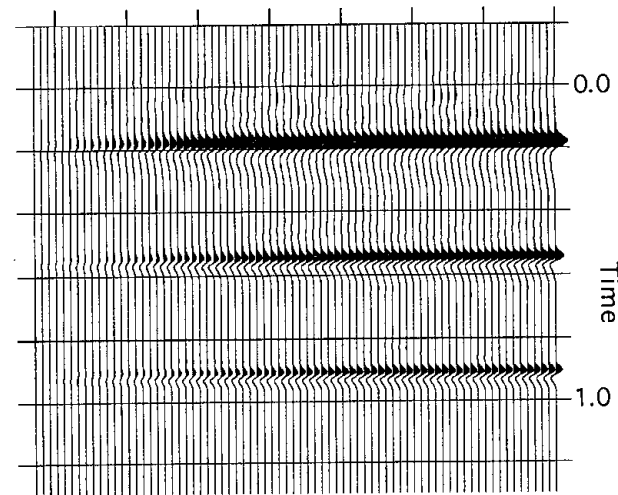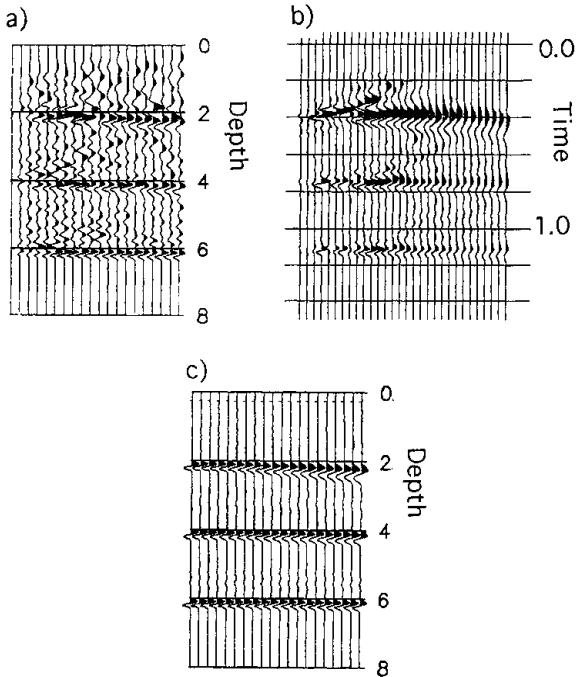

Fig. 4. Result of 3-D DMO and stack using the coordinates of the real 3-D survey (@ line A).

a)

b)

c)

Fig. 5. (a) One common image gather after 3-D prestack Kirchhoff migration using the real survey coordinates. (b) One CMP gather after 3-D DMO, PSI and NMO using the real survey coordinates. (c) One common image gather after 3-D prestack Kirchhoff migration of a regular survey.
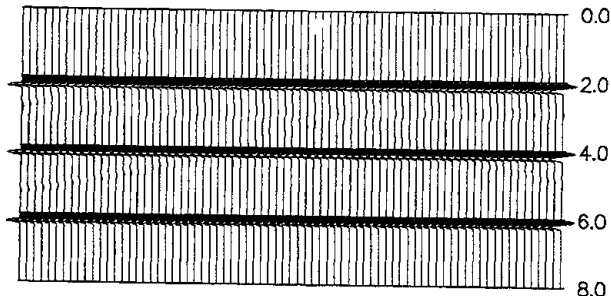
Fig. 6. (a) 3-D prestack Kirchhoff migration using a single fold, constant offset (2000 ft), constant azimuth, small regular spacing (55 ft).
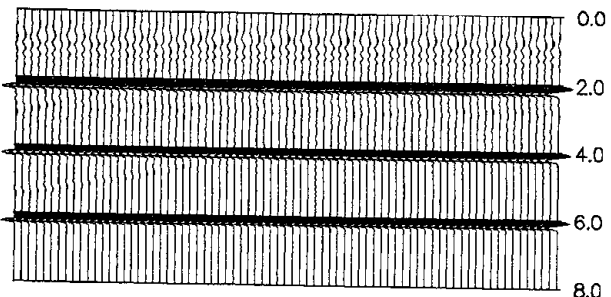
Fig. 6. (b) 3-D prestack Kirchhoff migration using a single fold, small regular spacing (55 ft) but small variation in offset (between 2000 A and 2400 ft).
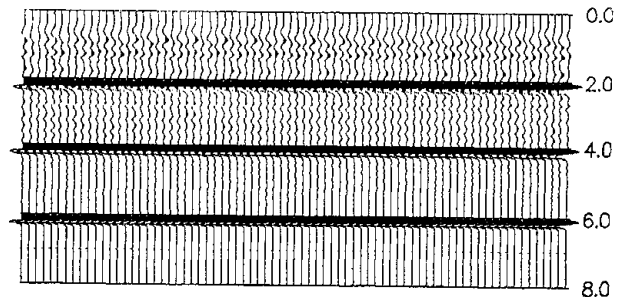
Fig. 6. (c) 3-D prestack Kirchhoff migration using a single fold, small regular spacing (55 ft) but large variation in offset (between 1990 ft. and 4300 ft).
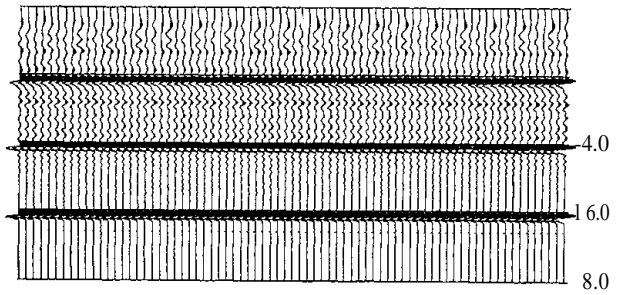
Fig. 6. (d) 3-D prestack Kirchhoff migration using a single fold, large regular spacing (220 ft) but 16 fold.
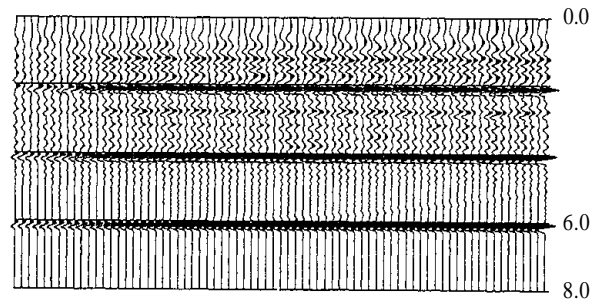
Fig. 6. (e) 3-D prestack Kirchhoff migration using a single fold, constant offset (2000 ft), constant azimuth, large regular spacing (220 R).
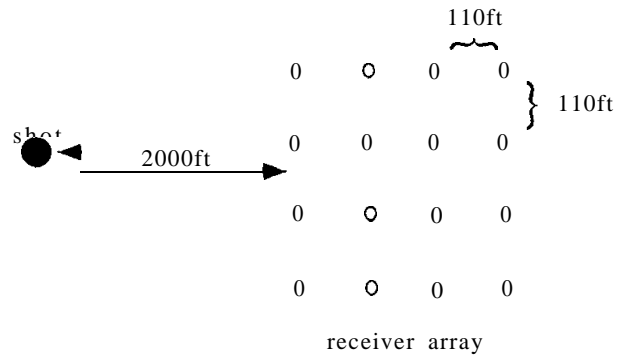
Fig.7: Template used to build a 3-D survey for Figure 6b.